Agriculture and Food

AIMS Agriculture and Food, 9(2): 445–471.
DOI: 10.3934/agrfood.2024026
Received: 09 December 2023
Revised: 09 April 2024
Accepted: 12 April 2024
Published: 18 April 2024

http://www.aimspress.com/journal/agriculture

Research article

Proteins of the food-borne pathogen *Listeria monocytogenes* strain F2365 relevant to lethal acidic stress and during rapid inactivation

Donglai Zhang[1,*], Zongyu Liu[1], Mingchang Jia[1] and John P. Bowman[2]

[1] Department of Chemical Engineering, Hebei Petroleum University of Technology, No. 2, Xueyuan Road, High Tech Industrial Development Zone, Chengde City, Hebei Province, 067000, P.R. China

[2] Centre for Food Safety and Innovation, Tasmanian Institute of Agriculture, University of Tasmania, Hobart, Tasmania, Australia

* **Correspondence:** Email: zhangdl2156256@hotmail.com.

Abstract: *Listeria monocytogenes*, which causes human listeriosis after consumption of contaminated food, can adapt and survive under a wide range of physiological and chemical stresses. In this study, the overall proteomic response of the *L. monocytogenes* strain F2365—a strain with mutations limiting its ability to tolerate acidic conditions—to progressive non-thermal acidic inactivation was investigated. The challenge process was investigated in the early stationary growth phase where F2365 cultures were acidified (pH 3.0, HCl) at 5 min, 1 h, and 2 h, generating pH 4.8, pH 4.1, and pH 3.5, respectively, with protein abundance measured using iTRAQ. Approximately 73 proteins increased in abundance and 8 declined when acidic stress became non-growth-permissive (pH < 4.1) and inactivation accelerated to approximately 2 log units/h. The functional categories of responding proteins were broad but the proteins involved were specific in nature and did not include whole pathways. Many responses likely accentuate energy conservation and compensate vital metabolic processes. For example, further repression of FlaA, normally repressed under acidic stress, occurs accompanied by an increase in quinol oxidase subunit QoxA and glycerol kinase GlpK. Proteins maintaining cell wall integrity, such as Iap and CwlO, manifested the overall largest abundance increase trend. Virulence proteins were also induced, including InlA, InlC, Hyl, Mpl, PlcA, and PlcB, suggesting that acidification may have mimicked conditions inducing some host survival traits. The overall suite of proteins affected appears to be the “last ditch” responses to non-thermal inactivation above and beyond the standard protections afforded in the stationary-growth phase. The array of proteins found here may provide a deeper understanding of the

physiological responses of this pathogen during non-thermal inactivation.

Keywords: *Listeria monocytogenes*; inactivation; time course; iTRAQ; acid tolerance

1. Introduction

As a potentially fatal food-borne pathogen, the Gram-positive bacterium *Listeria monocytogenes* threatens public health as well as the food industry. This pathogen is known for its ability to survive harsh environments, for instance non-growth-permissive acidic conditions including the mild fermentation–based preservation processes used for many low-pH foods, such as fermented meat, cheese, orange juice, salad dressing, and yogurt. *L. monocytogenes* infection can lead to gastroenteritis, meningitis, encephalitis, mother-to-fetus infections, and septicemia in immunocompromised individuals, pregnant women, and newborns, with a mortality rate of nearly 28% [1–4].

Proteomic-based approaches have been applied to better understand the mechanisms of *L. monocytogenes* response to a wide range of physiological stressors relevant to food preservation, processing, and sanitation of food production facilities. Stressors assessed include mineral and organic acids, salt, cold, heat, alkaline substances, detergents, oxidative chemicals, organic antimicrobials, and high hydrostatic pressure (e.g., [5–7]). Proteomics has revealed that cellular responses to stress can be complex. By measuring relative protein changes by methods such as iTRAQ technology, proteomic profiles can provide useful information about manifested phenotypes linked to protein function, metabolic pathways, and regulatory networks.

The response to acidic stress in isolation mainly affects the biochemical processes related to managing oxidative stress and energy production, nutrient uptake, and cell envelope integrity. The effects on cells are highly temperature-dependent [8–11]. Understanding the extent to which proteins form and how they merge to form a functional unit in order to cope with environmental stress also provides relevant information for understanding how organisms respond to different scenarios, particularly over short timescales and when in specific physiological contexts. Furthermore, the understanding of pathogen metabolism to stress can be achieved by reconstructing metabolic pathways and understanding de novo end-product metabolite formation such as lipids, proteins, and high-energy intermediates. The complexity during stress response and adaptation arises because stress-related proteins are involved in a variety of cellular activities including gene regulation, intermediary metabolism, compatible solute uptake, protein folding, ATP-dependent proteolysis, and DNA repair. Proteome data can be best interpreted to provide indications of the following: i) which responses lead to adapted physiological states (phenotypes), which requires prior knowledge of the related proteins; ii) responses that are more compensatory in nature, and so maintain the cellular status quo and not a new phenotype; and iii) the main regulatory networks, which requires knowledge of the associated regulons. Proteomic studies have shown that prior adaptation of *L. monocytogenes* to mild (growth-permissive) acidic conditions increases the tolerance of cells to more severe acid stress [10]. Furthermore, high but growth-permissive temperatures induce cross-protection against acidic and other stressful conditions [12,13]. In both of these situations, abundances of proteins change to ensure maximal cell wall stability, osmotic control (via osmolyte uptake transporters), cytoplasmic homeostasis, overall proteostasis (avoiding protein aggregation),

and cytoplasmic membrane integrity [12]. Disruptions to energy production and depletion of cell ATP pools are typical effects of acid stress and indirectly lead to membrane and cell wall damage, uncontrolled protein aggregation, and subsequent cell death. Depending on the nature of energy availability hurdles, *L. monocytogenes* can compensate by increasing carbohydrate metabolism [13], while altering ATP synthesis helps to maintain some ATP. It was found that once ATP drops below a critical threshold, cells become permanently inactivated (dead).

In the present study, we aimed to identify differentially expressed proteins where *L. monocytogenes* was exposed to different pH during the early stationary growth phase (pH 4.8, 4.1, and 3.5, adjusted using HCl) and forced into a process leading to a state that was unrecoverable. Rapid changes in protein abundances that occur due to the imposed acid stress were quantified using iTRAQ techniques with the aim of obtaining new insights into the cellular response strategies developed by *L. monocytogenes* to survive in non-growth permissive low-pH stress conditions. The milder pH levels studied cross the boundary of growth permissiveness of *L. monocytogenes,* which grows down to pH 4.2–4.3 in rich organic media at 25 ℃ [14]. In previous studies, we observed that temperature is the main factor that governs the inactivation rate of vegetative bacteria under growth-preventing conditions [15] and that underlying this is an array of responses that are dynamic, complex, and interconnected by regulatory processes [8,10]. By examining the responses of *L. monocytogenes* to growth/no growth boundary pH conditions, the goal is to determine whether there is a window for protein synthesis to aid survival and also determine the extent of this capability at the lethal side of the growth/no growth boundary. There is a tendency for *L. monocytogenes* to show complex inactivation responses also due to inherent physiological variation in its cell populations. We have observed previously that a small proportion of cells (depending on the temperature) can survive non-growth-permissive acidic conditions potentially over an extended time. This survival increases at lower temperatures [8,15]. The experiments also seek to understand what traits may be linked to these survivor sub-populations. One major hurdle is the strain choice, as *L. monocytogenes* does not exhibit homogenous responses to acid stress; thus, choosing a representative strain does not cover the extent of diversity of the species [10]. To overcome this, the decision was to examine acid stress in a strain that is more vulnerable to acid chemical exposure, which is a factor that complicates acid adaptation in *L. monocytogenes*. The experiments were thus performed using the strain F2365. Due to stop codon mutations, this strain has a moderately impaired ability to tolerate acid and oxidative stress and also cell invasiveness [16,17]. The mutations likely weaken its cell wall envelope integrity compared with other *L. monocytogenes* strains such as ScottA [10]. This makes F2365 slightly more vulnerable to infiltration of protons during acid shock; otherwise, its acid tolerance response seems fully intact. This study helps to determine what other traits are key to acid stress survival, besides those that are linked to the stationary growth phase or influenced by other stress responses. Understanding the lethal and sub-lethal effects of acid stress will deepen our understanding of the survival of the pathogen *L. monocytogenes* in acidic foods and food production facilities. Such knowledge can be informative in developing new approaches that intervene against and control *L. monocytogenes* contamination in susceptible food products.

2. Materials and methods

2.1. Bacterial cultivation and acid pH inactivation

L. monocytogenes strain F2365 was routinely grown using tryptone soya broth supplemented with 0.6% yeast extract (TSB-YE, Oxoid, Beijing, China) at 37 ℃. For inactivation treatments, strains were grown to the early stationary growth phase (12 h incubation at 37 ℃ in a shaking water bath, 100 rpm) in 1 L of TSB-YE broth, and filter-sterilized HCl (pH 3.0) was gradually added to the culture; at pH 4.8, 4.1, and 3.5, samples were taken. Cultures pelleted were centrifuged and plate-counted by using brain heart infusion agar supplemented with 0.1% pyruvate (BHA-P) to determine the culturable cell population. These experiments were performed in triplicate.

2.2. Protein extraction

We followed the method of [18]: 1 g of wet weight of cell pellet from each sample, including three independent biological replicates, were washed with phosphate-buffered saline (PBS) (pH 7.4), to remove flocculent precipitation; then, samples were dissolved in 1/10 volumes of SDT buffer (4% SDS, 100 mM DTT, and 150 mM Tris–HCl at pH 8.0). After 3 min incubation in boiling water, the suspensions were ultrasonicated with 10 rounds of 80 W sonication for 10 s with 15-s intervals. The crude extract was clarified by centrifugation at 13,000 × g at 20 ℃ for 15 min. Protein concentration was determined using the Bicinchoninic acid (BCA) Protein Assay Kit (Promega, USA), and supernatants were stored at −80 ℃ until further analysis.

2.3. Protein digestion and iTRAQ labeling

Protein digestion was performed according to the filter-aided sample processing (FASP) procedure, as described previously [19]. In brief, 200 μg of proteins in each sample was added to 30 μL of SDT buffer (4% SDS, 100 mM DTT, 150 mM Tris-HCl at pH 8.0). Detergent, DTT, and other low-molecular-weight components were removed by UA buffer (8 M urea, 150 mM Tris-HCl at pH 8.0) by repeated ultrafiltration (Pall units, 10 kD). After addition of 100 μL of iodoacetamide (50 mM in UA), samples were shaken at 600 rpm for 1 min, incubated in the dark for 30 min, and then centrifuged at 13,000 × g for 10 min. Filters were washed three times with 100 μL of UA buffer and two times with 100 μL of DS buffer (50 mM triethylammonium bicarbonate at pH 8.5). Protein suspensions were digested with 2 μg of trypsin (Promega, USA) in 40 μL of DS buffer at 37 ℃ for 16 h. Resulting peptides were collected as the filtrate. Peptide concentration was determined by UV light spectral density at 280 nm from an extinction coefficient of 1.1 of 0.1% (g/L) solution.

The resulting peptide was labeled using the 4-plex iTRAQ reagent according to the manufacturer's instructions (Applied Biosystems, California, USA). Each iTRAQ reagent was dissolved in 70 μL of ethanol and added to the respective peptide mixture. Samples were then labeled as (C)-113, (T1)-114, (T2)-115, or (T3)-116, with three independent biological replicates. Samples were incubated for 2 h at room temperature and, after terminating the labeling reaction, the labeled samples were mixed and vacuum dried.

2.4. Strong cation exchange (SCX) chromatography

The labeled samples were separated by SCX chromatography using the AKTA Purifier system (GE Healthcare, Fairfield, CT, USA). Briefly, the dried peptide mixture was reconstituted in 2 mL of buffer A (10 mM KH_2PO_4 in 25% of CAN at pH 2.7) and loaded onto a PolySULFOETHYL 4.6 × 100 mm column (5 μm, 200 Å, PolyLC Inc, Maryland, USA). The peptides were then eluted at a flow rate of 0.9 mL/min with a gradient of 0%–10% buffer B (500 mM KCl, 10 mM KH_2PO_4 in 25% of CAN at pH 2.7) from 0 to 2 min, 10%–20% buffer B until 27 min, 20%–45% buffer B until 32 min, and 50%–100% buffer B until 37 min. The elution was monitored at 214 nm, and fractions were collected every minute for a total of 35 fractions. The collected fractions were then combined into 10 pools and desalted on C18 cartridges (66872-U, Sigma, USA). Each fraction was vacuum freeze dried by vacuum centrifugation and reconstituted in 40 μL of 0.1% (v/v) trifluoroacetic acid.

Finally, all samples were kept at −80 ℃ until further analysis.

2.5. LC–MS/MS analysis

Experiments were analyzed on a Q Exactive mass spectrometer coupled to an Easy nLC system (Thermo Fisher Scientific, Waltham, MA, USA). For nano LC-MS/MS analysis, 6 μL of each fraction was injected. The peptide (5 μg) was loaded onto a Thermo Scientific EASY column (2 cm × 100 mm, 5 mm C18) using an autosampler. Peptides were eluted onto an analytical Thermo Scientific EASY column (75 mm × 100 mm, 3 mm C18) and separated with a linear gradient of buffer B (0.1% formic acid and 80% acetonitrile) at a flow rate of 250 nL/min over 60 min.

Mass spectrometry data were obtained in peptide recognition mode using a survey scan of 300–1800 m/z for the 10 most abundant precursor ions after high-energy collision disfragmentation.

The duration of the dynamic exclusion was 50 s. The measured scans had a resolution of 70,000 at m/z 200 and the resolution for HCD spectra was set at 17,500 at m/z 200. The normalized collision energy was 30 eV, and the underfill ratio was defined as 0.1%. The instrument was run with the peptide recognition mode enabled.

2.6. Sequence database searching and data analysis

The raw data of mass spectrometry were searched using MASCOT engine (Matrix Science, London, UK; version 2.2). The MASCOT engine was embedded into Proteome Discoverer 1.4 (Thermo Electron, San Jose, CA) against the UniProt *Listeria* database (268,763 sequences, download at 08/08/2014) and the Decoy database. The following search parameters were used for protein identification: peptide mass tolerance 20 ppm, MS/MS tolerance 0.1 Da, enzyme trypsin, missed cleavage 2, fixed modified carbamidomethyl (C), iTRAQ 4-plex (K), and iTRAQ 4-plex (N-term), variable modification oxidation (M). All reported data were based on a false discovery rate (FDR) of less than 1% confidence for protein identification.

2.7. Bioinformatics

The Gene Ontology (GO) program Blast2GO (https://www.blast2go.com/) was used to annotate differential expression proteins (DEPs) to create histograms of GO annotation, including biological

process, cellular component, and molecular function [20,21]. For pathway analysis, the DEPs were mapped to the terms from KEGG (Kyoto Encyclopedia of Genes and Genomes) [22] database using the KAAS program (http://www.genome.jp/kaas-bin/kaas_main). Protein–protein interaction networks were analyzed using the publicly available program STRING (http://string-db.org/) with the required minimum interaction score set to 0.400.

2.8. Parallel reaction monitoring (PRM) analysis

To further check the levels of protein expression gained through label-free analysis, additional quantification through LC-PRM MS analysis [23] was applied. Briefly, the iTRAQ protocol was used for peptide preparation. The stable isotope AQUA peptide was spiked in each sample and used as a standard internal reference. Tryptic peptides were loaded on stage tips of C18 for desalting prior to reversed-phase chromatography on one of the nLC-1200 easy systems (Thermo Scientific). Then, 1 h liquid chromatography gradients were performed with 5%–35% acetonitrile for 45 min. Q Exactive MS was applied for PRM analysis. Optimized methods for measuring the energy of collision, state of charge, and retention time of the most crucial peptides were gained from experiments involving unique peptides with high intensities; therefore, each targeted protein could be handled properly. The analysis of raw data was realized via Skyline (MacCoss Lab, University of Washington) [24], wherein the intensity of signal produced by a certain peptide sequence could be quantified with respect to each sample and referenced to standards via normalization for each protein.

3. Results and discussion

Previous studies have performed proteomics analyses on *L. monocytogenes* exposed to single- and multi-stress (e.g., acid and salt) conditions. Acid stress is imposed by exposure to mineral acids, organic acids, or both [6–8,10,12,25–27]. However, extending from these studies, the proteome of *L. monocytogenes* in response to progressive mineral acid exposure in a time course experiment focusing on the strain F2365 provides an opportunity to explore the boundaries of acid stress survival in tandem with relatively rapid inactivation (cell death). F2365, a 4b serotype (lineage I) strain as tested here has a reduced ability to tolerate acid stress due to stop codon mutations [17]. Research performed on other strains, such as ScottA (4b serotype strain), shows that they can mount an extensive defense to acidic conditions, even with other stressors present (such as extreme osmotic stress), depending on the ambient temperature [8]. The experiment thus allows a comparison to "tough" strains, such as ScottA. The experiments utilized stationary growth phase cells. In that respect, standard defenses arising from the general stress response, induced when entering the stationary growth phase—which included heat shock proteins and oxidative stress management proteins—would be maximally activated, as these were not detected in the iTRAQ data obtained here. What is shown here are the specific responses to non-thermal stress above and beyond stress responses that enable rapid adaptation and cross-protection in *L. monocytogenes*, critical for host and external environmental survival. The focus of the experimental strategy is placed on responses that essentially precede a permanent inactivation state. It is important to note that studying a single strain will not capture the extent of responses that may occur in the full diversity of *L. monocytogenes*. Rather, the observations here are specifically targeted to explore responses of the highly studied

species and relatively genetically diverse *L. monocytogenes* to inactivation scenarios, which we have previously explored [8,28] to better understand food-borne pathogen death kinetics and its underlying physiological and molecular basis.

The complex effects of organic and mineral acids on cell survival and gene expression response, underlying inactivation that is non-linear (as described extensively in [8]), seem to relate to the ability of cell populations to maintain cytoplasmic membrane integrity and thus cytoplasm homeostasis. The loss of integrity in the cell wall and cytoplasm is highlighted by a depletion of cytoplasmic ATP accompanied by a decrease in the intracytoplasmic pH [29]. The rapidity of these changes and the associated rate of cellular inactivation can affect the ability to detect changes in protein expression due to loss of proteostasis, protein aggregation, and collapse of the intricate networks of protein interactions enabling life [30,31]. Proteostasis is the basic function in cells that maintains protein integrity by rescuing and refolding proteins or disposing of proteins that cannot be recovered. This is an energy-intensive process [32], and when it fails it heralds the inevitable death of the cell. In the experiments here, we assume this process is at its limit since there is likely no ATP to spare, and abundances of proteins involved in proteostasis are at maximal levels. Thus, slow changes in pH were used to avoid the rapid collapse of F2365's ability to cope with acid stress. Even extreme acidophiles, which possess multiple copies of highly conserved proteins involved in key steps of protein disaggregation and proteostasis (such as DnaK, DnaJ, GroEL/GroES, ClpP, Lon, FtsH, HtrA, Hsp20, SurA, and RidA) possess an upper boundary for resilience to protons infiltrating the cytoplasm, indicative of a hard boundary for life in this respect [33].

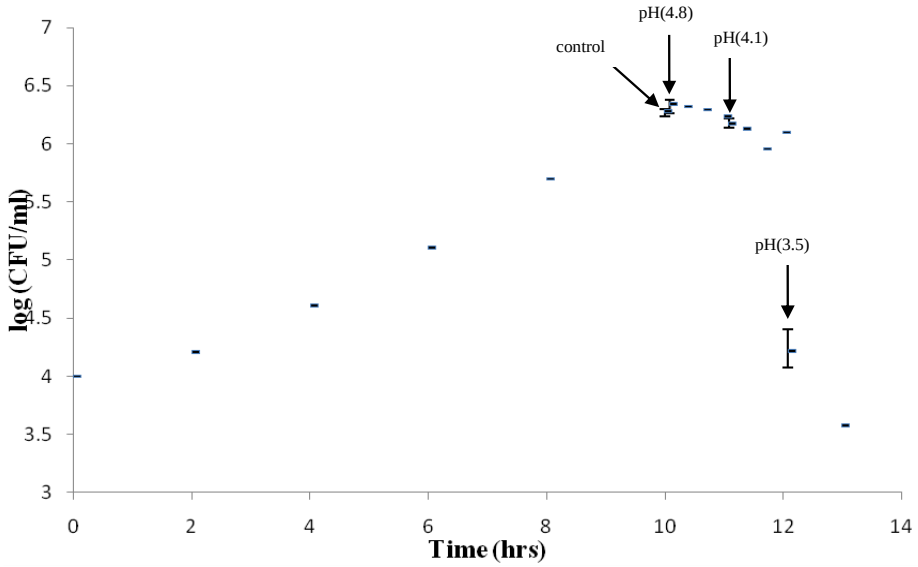

Figure 1. Sampling design for the study. The graph shows the viable populations of *Listeria monocytogenes* F2365 grown in TSB-YE at 37 ℃ to early stationary growth phase (starting at approximately 10 h). The pH of the medium was adjusted slowly by adding small volumes of a pH 3.0 HCl solution. The control was not exposed to any HCl and was collected at 0 min. For acid stress treatments, samples were collected after 5 min, 1 h, and 2 h, when pH had shifted to 4.8, 4.1, and 3.5, respectively, by HCl addition. The viable count was estimated by plate count immediately after collection of each sample. Cell samples were also analyzed for protein profiles via the iTRAQ approach.

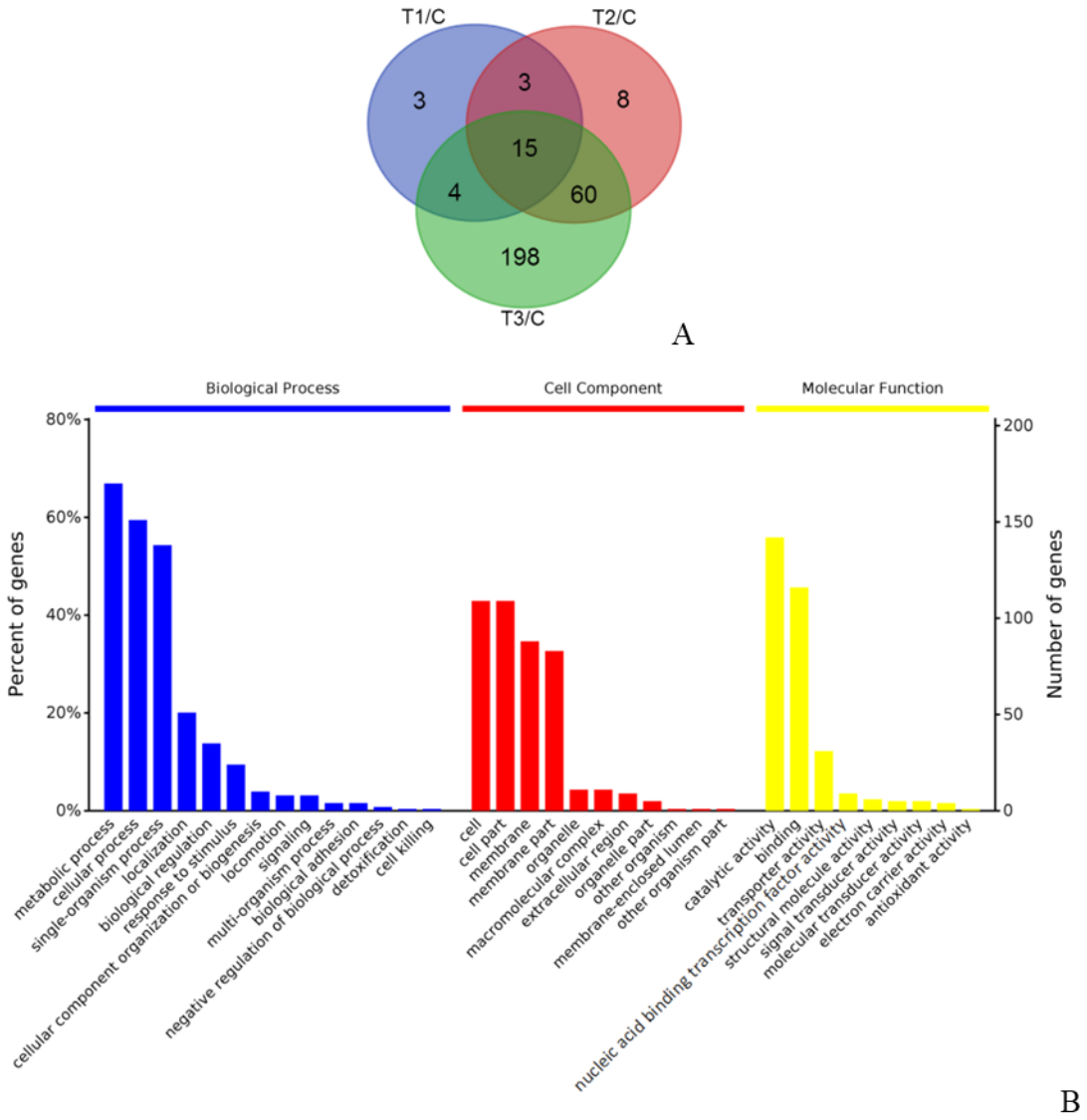

Figure 2. A. Venn diagram showing the number of proteins that changed significantly in abundance at the different time points following acidification (T1: 5 min, pH 4.8; T2: 1 h, pH 4.1; T3: 2 h, pH 3.5) of the medium (TSB-YE, 37 ℃) in which *Listeria monocytogenes* F2365 had reached early stationary growth phase. The changes are relative to the 0-time control sampled before acidification commenced. B. The distribution of broad functional responses as defined through ontology for significantly responsive proteins across all treatments combined.

To ensure the accuracy of the proteome information, the F2365 cell viability was enumerated at each sampling time, and culture purity was confirmed before proteomics analysis as shown in Figure 1. The mean viability of early stationary growth phase *L. monocytogenes* F2365 was 6.27 log CFU/mL. Cells were then exposed to a solution of pH 3.0 (HCl). At 5 min sampling at pH 4.8, the mean viability was 6.34 log CFU/mL; at the 1 h sampling time, pH had dropped to 4.1 and the mean count was 6.16 log CFU/mL. Further HCl addition reduced the pH to 3.5 by the 2 h mark, well below the point of growth permissiveness [14]. At this point, inactivation was rapid with the mean viability

declining almost 2.06 log units to 4.21 log CFU/mL. For the sample point at pH 4.8, changes in population viability were negligible, while at pH 4.1 the 0.2 log unit viability loss (compared to the 0 time control) appears to herald that cell decline was starting to occur. The inactivation process (death kinetics) requires time, and it is assumed that most of the viability loss occurs once a boundary of cellular acid tolerance has passed. At 37 ℃, this appears to be around pH 4.2 [14]; thus at 1 h the inactivation was only just beginning, and between 1 h and 2 h the rate of death had likely become log-linear. This would be consistent with previous findings [8,15], where the size and continued viability of the cell population depends on the temperature during inactivation and the loss rate accelerates with temperature increase.

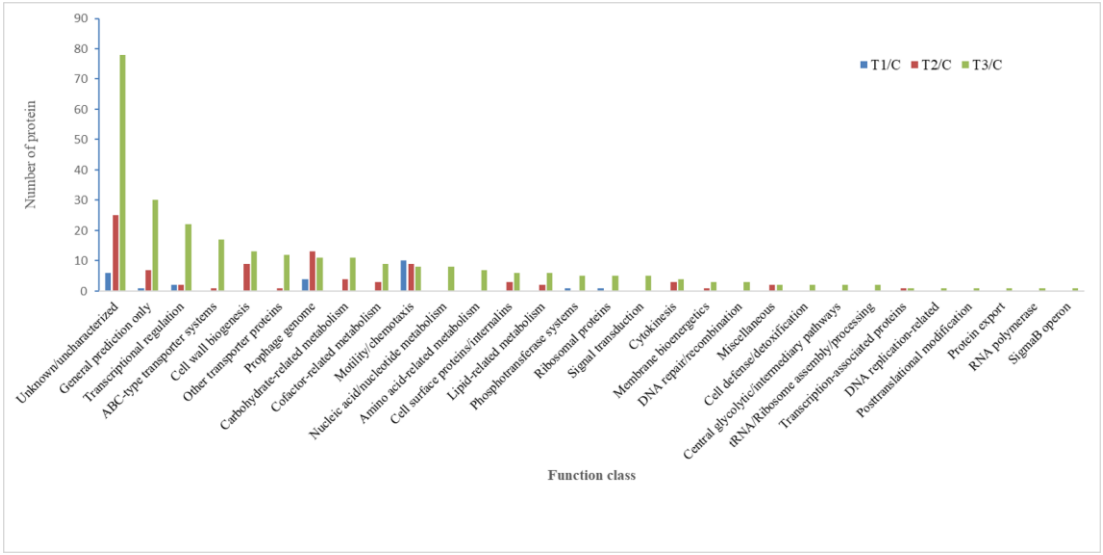

Figure 3. Effect of progressive medium acidification (adjusted with HCl solution of pH 3.0. T1: 5 min, pH 4.8; T2: 1 h, pH 4.1; T3: 2 h, pH 3.5) on *Listeria monocytogenes* F2365 grown in TSB-YE at 37 ℃. Responses shown are the number of proteins significantly affected, assigned to functional groups based on ontology.

To better understand the underlying response mechanisms of *L. monocytogenes* to progressive acidic shock, this study used iTRAQ technology to examine genetic and protein changes in *L. monocytogenes* from the same samples described above to determine their viability. The raw data were then analyzed using MASCOT, and the proteins were quantified. From the iTRAQ 4x-plex experiments, a total of 2131 proteins were identified. Of these, 291 proteins generated had a significant difference in abundance (≥ 1.20 or ≤ 0.83 fold change, $p < 0.01$), while 90 proteins were in the range ≥ 1.50 or ≤ 0.67 fold change. A Venn diagram shows the details of the overlap between treatments and the proteins unique to each processed dataset (Figure 2A). A total of 15 proteins significantly changed in abundance at all treatment points. Table 1 lists the proteins showing both significant ($p < 0.01$) and sizable changes (≥ 1.50 or ≤ 0.67 fold change). Enrichment analysis of these proteins based on GO terms is shown in Figure 2B. Among the proteins that underwent significant changes, the GO terms of level 2 associated with 34 GO categories were found. The 14 GO term groups were based on derived biological processes, including metabolic, cellular, and single-biological processes. Effects could be linked to cellular components, mainly including the

whole cell, cell wall, and cell membranes, as well as to molecular functions, including catalytic activity and binding. These results suggest that responses are quite global in nature, affecting many aspects of the cell down to specific enzyme functions.

In Figure 3, which shows GO terms grouped by timepoint, and in Figure 4, which is a heat map showing specific protein responses, it is visible that the most dramatic changes in protein abundances occurred at the time point (2 h) at which pH 3.5 was achieved. This includes proteins having reduced and increased abundance, with a skew to the latter (Figure 4). By comparison, very few proteins change with pH 4.8, and a moderate number change at pH 4.1. The results demonstrate that F2365, even though lacking an ATR, still mounts a response to acid stress and has an inherent acid tolerance up to around pH 4.1. Clearly beyond the range of growth-permissiveness, this capacity collapses and, from former studies, inevitably leads to cell death [8].

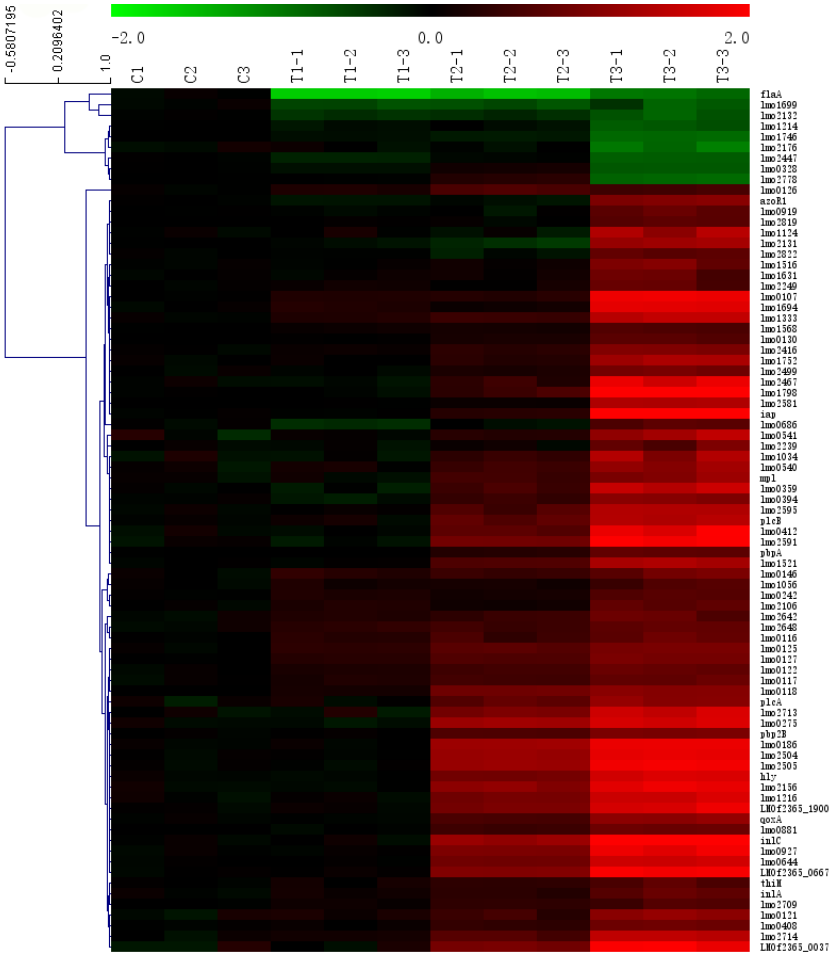

Figure 4. Heat map showing the changes in abundance (green: decreased, red: increased) of proteins responding to progressive medium acidification (adjusted with HCl solution of pH 3.0. T1: 5 min, pH 4.8; T2: 1 h, pH 4.1; T3: 2 h, pH 3.5) on *Listeria monocytogenes* F2365 grown in TSB-YE at 37 ℃. The results demonstrate that acidification causes a skew toward an overabundance of proteins. Protein designations are based on the homologs of the highly characterized strain *Listeria monocytogenes* EGD-e.

In order to reveal the interaction network associated with low pH stresses towards early stationary phase *L. monocytogenes* F2365, a protein–protein interaction (PPI) network was constructed using the STRING protein–protein interaction database, KEGG pathway, and GO biological process analyses (Supplementary Figure S1). Protein names were represented by the names or locus numbers of the homologous proteins in *L. monocytogenes* EGD-e in the PPI map and were included in Table 1. The nodes of the network show proteins that interact over 14 categories, including transcriptional regulation, ribosomal proteins, nucleic acid/nucleotide metabolism, amino acid–related metabolism, ABC-type transporters, central glycolytic/intermediary pathways, lipid-related metabolism, membrane bioenergetics, prophage genome, phosphotransferase systems, cell wall biogenesis, and other transporter proteins, as well as proteins that have a function that is only a generalized prediction (based on conserved domains) or that is uncharacterized.

The proteomic results were in accordance with the verification analysis by parallel reaction monitoring (PRM) assays (Table 2). The expression levels of 15 candidate proteins with potential salt-tolerant functions were chosen for quantification by PRM to verify the iTRAQ results. The Pearson correlation coefficient between iTRAQ and PRM results was $R^2 = 0.67$ ($p < 0.01$), showing that these results had a significant correlation. In general, all proteins detected by PRM had changes that were consistent with the iTRAQ quantification results. Our PRM assay illustrated that iTRAQ results were credible as a means of analysis.

Changes in protein abundance due to acidic stresses were determined by comparing the profiles obtained after the shift to that of a reference sample taken prior to the shift. Table 1 and Figure 4 include complete lists of the number of proteins with significant abundance changes from each treatment. To investigate a possible interdependence of the proteins within functional groups and to visualize their expression patterns under low pH stress, we performed hierarchical clustering to find associated changes in the acid-responsive proteins as indicated in Table 1 and Figure 4. Two main clusters were observed in this cluster tree on the left side in Figure 4. It was found that the proportions for upregulated proteins were greater than for downregulated proteins. The progressive sub-lethal to lethal acidic shock, even without an overlayed ATR, results in a response involving a dispersed range of proteins (Table 1, Figures 3 and 4) and affects multiple metabolic pathways (summarized in Figure S2). In Figure 3, several functional categories are enriched with proteins with significant abundance changes. Broadly, these proteins include ABC-type transporters involved in specific aspects of amino acid and carbohydrate-related metabolism, cell surface proteins/internalins including several proteins of the main pathogenicity island LIP1 (Hyl, Mpl, PlcB) as well as InlA and InlC (but not InlB, the gene for which is a pseudogene in F2365), cell wall biogenesis and co-factor-related metabolism, cytokinesis, lipid-related metabolism, membrane bioenergetics, motility/chemotaxis, nucleic acid/nucleotide metabolism, associated with a conserved prophage remnant (lmo0114-lmo0128), and specific transcriptional regulators but excluding master regulators responsive to stress (i.e., SigB, CodY, HtrA).

Amongst ABC-type transporter systems, Lmo1746 (VirA) was downregulated, while Lmo0919 (VgaL), Lmo2499, Lmo0541, Lmo2581, and Lmo0107 were upregulated. VirA contributes to LiaR-mediated salt-induced nisin resistance and virulence and could be linked to cell wall stability [34]. On the other hand, VgaL and Lmo0107 are part of different efflux complexes likely conferring resistance to certain macrolides (lincosamide, streptogramin A) or other unspecified toxic metabolites [35,36]. The other induced transporter proteins are instead involved in inorganic phosphate (Lmo2249), iron complex (Lmo0541), and heme (Lmo2581) uptake. The upregulation of

heme-degrading enzyme Lmo0484 [37] also suggests that the response is geared toward either iron extraction or precursors for heme synthesis. Though the findings for antimicrobial resistance are not interpretable, there seems to be some evidence that F2365 attempts to compensate acid shock by phosphate, iron, and heme uptake. All of these resources would be useful in combating the oxidative damage derived from acid stress and conceivably compensate or bolster levels of protective heme-containing enzymes such as catalase, as well as aiding proton extrusion via ATPase, a process that requires phosphate for ATP synthesis and for replenishment of other processes, depending on phosphorylation reactions [10,29]

Relevant to amino acid–related metabolism, only Lmo2819 and TrpD were upregulated. The M20 family carboxypeptidase Lmo2819 is uncharacterized and whether it has specific protein targets is unknown. TrpD (anthranilate phosphoribosyltransferase) is a phosphate-dependent enzyme needed to generate the phosphoribosyl anthranilate intermediate [38]. This could suggest that tryptophan synthesis is a bottleneck for proteostasis. Though not studied in bacteria, tryptophan has been shown to have some importance in delaying protein aggregation [39].

Carbohydrate-related-metabolism proteins showing increased abundance included glycerol kinase GlpK (Lmo1034), class II fructose bisphosphate aldolase FbaA (Lmo0359), and chitin-binding protein (Lmo2467), all upregulated. These proteins have multifunctional roles, some of which are yet to be understood. GlpK is needed to activate glycerol for catabolism and is used purely for energy supply [40]. FbaA has a central role in both glycolysis and gluconeogenesis and is also expressed on the surface of cells [41]; thus, besides enabling energy production, this enzyme mainly shows a moonlighting role [42] of unknown nature, which could though be linked to stress survival. For Lmo2467, its role as a chitin-binding protein has been shown, but it is also needed for host survival although no chitin is available in human hosts [43]. This suggests that Lmo2467 has another role, which is stimulated under acid-stress conditions like FbaA. The results indicate specific responses and not wholesale increases in pathways, for example for synthesis of building blocks or catabolism. Glycerol is generally more available in human host cells, so F2365 could be geared to that substrate in the advent of energy stress brought about by acid exposure, as would occur in macrophage phagosomes. ThiM (thiaminase) was observed to have increased abundance; this change could suggest salvage of thiamine increases [44]. FbaA is a thiamine and phosphate-requiring protein; ThiM protein may act to keep thiamine readily available for FbaA function. Also relevant to energy generation and membrane bioenergetics, the AA3-600 quinol oxidase subunit QoxA had increased abundance. It is presumed that the quinol oxidase complex enables *L. monocytogenes* to generate energy within host cells [45]; thus, an increase in the activity of this complex could be compensatory for lower electron transport chain activity due to the high external proton concentrations. Typically, the quinol oxidase complex has quite low abundance under standard growth conditions, as *L. monocytogenes* relies largely on heterofermentation for ATP synthesis including when under growth-permissive acidic conditions [10].

Proteins in the LPI1 (PlcA, PlcB, Hyl, Mpl) and LIP2 (InlA) pathogenicity islands and also InlC (internalin C) were upregulated. These proteins confer the means for host cell attachment, invasion, cell-to-cell spread, and also, via InlC, immune system subversion [46]. Data indicate that the increased InlA and InlC abundance is accompanied by an increase in the main sortase (SrtA, Lmo2714) that organizes and binds internalins to the outer region of the peptidoglycan layer [47]. Overall, this result is interesting since F2365, due to mutations, has lost the ability to invade host cells. This is partly due to disruption of the *inlB* gene [16]. It is possible that the rapid drop in pH

signals responses akin to gastric acid exposure and the presence of acidic conditions in the intestinal tract. PrfA, which activates LIP-1 and internal gene expression [3,4], is known to be controlled by temperature, suppressed by the availability of metabolizable carbohydrates, and activated by the availability of glutathione [48]. A specific experiment measuring intracellular glutathione concentrations is required to determine if this is linked to the acid stress response; however, no enzymes associated with glutathione were noted from the experiment. A simpler explanation is that available carbohydrates are simply depleted or not being metabolized. This is partly due to being in the stationary growth phase but could be due to a lack of proton motive force to drive the uptake of external carbohydrates. Depletion of sugar is known to transiently induce PrfA abundance and subsequent virulence gene expression [49], and thus the response for F2365 essentially harks to a response that energy flow in the cell has been disrupted.

Parallelling the increased abundance of sortase SrtA, numerous proteins associated with the cell wall and involved in its maintenance also became more abundant, as listed in Table 1 [i.e., PbpB, Lmo1216, Lmo0927, Lmo0186, Lmo2504, Lmo2505 (CwlO/Spl), Lmo2591, Iap (Lmo0582) and Lmo1798]. These proteins are either involved with peptidoglycan turnover and cell wall integrity (PpbB, Iap, CwlO/Spl, N-acetylmuramoyl-L-alanine amidases Lmo1216, Lmo1521, and Lmo2591) or with lipoteichoic acid synthesis [Fmt (Lmo0540), Lmo0644, Lmo0927, Lmo1798]. Cell wall–binding proteins Lmo0186 and Lmo2504 may also have a regenerative role in the cell envelope, but their exact function remains unclear [50]. Iap and CwlO/Spl are interesting in that they are required for viability and have key roles in managing peptidoglycan distribution, including the septation process of cell division. Acid stress may imbalance peptidoglycan synthesis (due to a lack of cell energy), and so these and the other proteins may act as a last means of maintaining cell wall integrity by recycling peptidoglycan. Disruption of the process could lead to complete loss of viability since cell division would be blocked and individual cells rapidly inactivate due to the degeneration of the cell envelope. Old *Listeria* cells can transit to L-forms [51], which are elongated, leaky, or autolyzed, as suggested by DNA leaking into the supernatant of cultures. These cells also are depleted in ATP and lack catabolic enzyme activity [52]. This phenomenon could be linked to the effects of cell wall–integrity disruption and loss of cytoplasmic homeostasis. To avoid protein aggregate accumulation [53], maintenance of proteostasis is needed as well as effective coordination of cell division, which allows continual redistribution of proteins within the cytoplasm.

As expected, acidic conditions suppress motility and chemotaxis. It is now well known that FlaA, the main flagella protein subunit [54], is extremely responsive to physiological stress—its abundance plunges when acid stress is applied at 25 ℃, a temperature in which cells are normally actively motile [10]. At 37 ℃, the levels of FlaA and cellular motility are much lower than at 25 ℃ due to the flagella synthesis being thermoregulated [55]; however, further reduction is expected since cells generate precursor flagella subunits to enable rapid responses to environmental change. Thus, lethal acid stress (pH 4.1 and 3.5), as applied here, likely eliminates both chemotaxis and adherence under non-growth-permissive acidic conditions.

Table 1. Whole proteome analysis of *Listeria monocytogenes* F2365 responses to acidic stresses at pH 4.8, 4.1, and 3.5.

F2365 Loci	EGD-e gene name	pH 4.8/C	Log ratio pH 4.1/C	pH 3.5/C	Known or predicted specific function
LMOf2365_2631	*lmo1034*	0.94	1.32	**2.43**	glycerol kinase
LMOf2365_0212	*plcA*	1.04	**1.65**	**2.15**	phosphatidylinositol-specific phospholipase C PlcA
LMOf2365_0148	*lmo0130*	1.02	**1.15**	**1.61**	putative cell surface anchored 5'-nucleotidase
LMOf2365_0136	*lmo0118*	**1.13**	**1.84**	**2.09**	putative phage tail protein, phage_tail_2_superfamily; antigen A protein LmaA
LMOf2365_0941	*lmo0919*	0.97	0.97	**1.68**	putative ABC transporter, ATP-binding protein
LMOf2365_1771	*lmo1746*	**0.93**	**0.87**	**0.57**	putative bacitracin (drug) efflux ABC transporter, permease protein
LMOf2365_2553	*lmo2581*	1	**1.06**	**2.59**	MacB-like ABC transporter, ATP-binding protein
LMOf2365_2810	*lmo2819*	1.02	1	**1.63**	putative N-acyl-L-amino acid amidohydrolase, M20_dimer superfamily
LMOf2365_1535	*lmo1516*	1	1.08	**1.92**	ammonium uptake transporter
LMOf2365_1653	*trpD*	1.03	1.08	**1.7**	anthranilate phosphoribosyltransferase
LMOf2365_0213	*hly*	0.97	**1.88**	**3.24**	membrane protein, HlyIII superfamily
LMOf2365_2165	*lmo2131*	0.94	0.77	**2.38**	putative Crp-like transcriptional regulator, CAP_ED superfamily
LMOf2365_2394	*lmo2423*	1.02	1.01	1.58	putative metal cation exporter, cation_efflux superfamily
LMOf2365_2694	*lmo2714*	1.11	**1.55**	**2.8**	putative cell wall sorted protein
LMOf2365_1723	*lmo1699*	**0.67**	**0.65**	**0.65**	methyl-accepting chemotaxis protein
LMOf2365_0722	*lmo0686*	**0.79**	0.94	**1.61**	flagellar motor rotation protein B
LMOf2365_2440	*lmo2467*	0.93	1.29	**3.44**	putative chitin binding protein, chitin_bind_3/FN3/chtBD3 superfamily
LMOf2365_0295	*lmo0275*	0.92	**2.38**	**3.22**	putative metallo-beta-lactamase superfamily protein
LMOf2365_2166	*lmo2132*	**0.77**	**0.79**	**0.62**	putative Crp-like transcriptional regulator, CAP_ED superfamily
LMOf2365_1718	*lmo1694*	1.2	1.09	**3.46**	putative nucleoside-diphosphate sugar epimerase, NADB_Rossmann superfamily
LMOf2365_1193	*lmo1183*	1.25	1.4	3.48	putative ethanolamine utilization-associated protein
LMOf2365_0726	*flaA*	**0.33**	**0.36**	**0.54**	flagellin Fla
LMOf2365_1816	*azoR2*	0.9	0.93	**2.05**	NADH-azoreductase, FMN-dependent
LMOf2365_0948	*lmo0927*	1.01	**1.98**	**3.64**	exported glycerolphosphate lipoteichoic acid synthetase
LMOf2365_0334	*thiM*	1.09	**1.29**	**1.57**	hydroxyethylthiazole kinase
LMOf2365_0471	*inlA*	1.1	**1.25**	**1.68**	internalin A; cell wall protein with LRR and B repeat domains InlA

Continued on next page

F2365 Loci	EGD-e gene name	pH 4.8/C	Log ratio pH 4.1/C	pH 3.5/C	Known or predicted specific function
LMOf2365_2282	*lmo2249*	1.09	1.06	**1.66**	low-affinity inorganic phosphate transporter
LMOf2365_1812	*inlB*	1.01	**2.29**	**4.44**	unanchored cell wall internalin B InlB
LMOf2365_0283	*inlE*	1.03	1.17	2.33	internalin E
LMOf2365_2178	*lmo2146*	0.96	1.01	0.65	putative transcriptional regulator, PBP2_CysL_like family
LMOf2365_0932	*lmo0910*	0.97	0.97	1.86	DUF1648 superfamily protein
LMOf2365_2272	*lmo2239*	0.96	1.04	**1.73**	uncharacterized protein
LMOf2365_0139	*lmo0121*	1.13	1.36	**2.18**	putative phage-associated membrane protein, COG5412 family
LMOf2365_0214	*mpl*	0.99	**1.41**	**2.11**	putative L-lactate dehydrogenase
LMOf2365_0125	*lmo0107*	**1.19**	1.22	**3.68**	putative export ABC transporter, ATP-binding/permease
LMOf2365_1540	*lmo1521*	1.01	**1.54**	**2.53**	N-acetylmuramoyl-L-alanine amidase
LMOf2365_1225	*lmo1216*	1.01	**1.89**	**3.11**	exoglucosaminidase/muramidase
LMOf2365_2568	*lmo2595*	1.03	**1.51**	**2.62**	uncharacterized protein
LMOf2365_1900		1.03	**1.94**	**3.39**	uncharacterized protein
LMOf2365_0570	*lmo0541*	1.02	1.23	**2.5**	iron complex uptake ABC transporter, substrate binding protein FecB-like
LMOf2365_0145	*lmo0127*	**1.24**	**1.54**	**1.91**	putative phage protein (Gp20 Listeria phage A118)
LMOf2365_0667		1.03	**2.04**	**3.86**	uncharacterized protein
LMOf2365_0162	*lmo0146*	**1.25**	**1.36**	**1.82**	uncharacterized protein
LMOf2365_0144	*lmo0126*	**1.17**	**1.52**	**1.44**	putative phage protein
LMOf2365_2195	*lmo2163*	1.02	1.02	0.63	putative dehydrogenase, GFO_IDH_MocA superfamily
LMOf2365_1457	*pbpA*	1	**1.23**	**1.68**	septal peptidoglycan transpeptidase
LMOf2365_2071	*pbpB*	1.02	**1.53**	**1.94**	septal peptidoglycan transpeptidase
LMOf2365_0569	*lmo0540*	1.09	**1.39**	**2.24**	cell division–associated peptidoglycan endopeptidase
LMOf2365_2477	*lmo2504*	0.99	**2.3**	**3.55**	putative murein endopeptidase
LMOf2365_2478	*lmo2505*	0.98	**2.31**	**3.81**	peptidoglycan DL-endopeptidase P45
LMOf2365_0406	*lmo0394*	0.89	**1.35**	**2.07**	Nlp/60 family protein
LMOf2365_0611	*iap*	0.99	**1.25**	**5.56**	gamma-D-glutamate-meso-diaminopimelate muropeptidase; invasion-associated protein Iap
LMOf2365_2472	*lmo2499*	0.98	1.16	**1.88**	phosphate ABC transporter, substrate binding protein

Continued on next page

F2365 Loci	*EGD-e gene name*	pH 4.8/C	Log ratio pH 4.1/C	pH 3.5/C	Known or predicted specific function
LMOf2365_0216	*plcB*	1.05	**1.65**	**2.66**	zinc-dependent phospholipase C PlcB
LMOf2365_2620	*lmo2648*	**1.27**	**1.39**	**1.69**	putative phosphotriesterase, metallo-dependent hydrolase superfamily
LMOf2365_1825	*lmo1798*	0.96	**1.39**	**6.27**	putative poly (glycerol-phosphate) alpha-glucosyltransferase
LMOf2365_1202	*cobH*	0.93	1.58	0.41	precorrin-8X methylmutase CobH
LMOf2365_0016	*qoxA*	0.98	**1.48**	**2.18**	AA3-600 quinol oxidase subunit II
LMOf2365_2139	*lmo2106*	**1.19**	1.09	**1.67**	putative phosphohydrolase, MPP_YkuE_C family protein
LMOf2365_2615	*lmo2642*	1.2	**1.35**	**1.7**	putative metal-binding phosphohydrolase, Icc superfamily
LMOf2365_0675	*lmo0644*	1.01	**1.84**	**3.07**	putative sulfatase or phosphoglycerol transferase, alkaline phosphatase superfamily
LMOf2365_2208	*lmo2176*	1	0.97	**0.53**	putative ArcR-like transcriptional regulator, TetR_N superfamily
LMOf2365_2420	*lmo2477*	0.83	0.97	**0.6**	putative transcriptional regulator, HTH_XRE/Rgg_CTERM superfamily
LMOf2365_0288	*lmo0269*	0.92	1.03	2.95	putative ABC transporter, permease
LMOf2365_1777	*lmo1752*	1.02	**1.23**	**2.49**	uncharacterized secreted protein
LMOf2365_1223	*lmo1214*	0.92	0.95	**0.63**	DUF2812 superfamily protein
LMOf2365_1350	*lmo1333*	**1.2**	**1.37**	**2.83**	putative secreted protein, YceG-like superfamily
LMOf2365_0135	*lmo0117*	1.17	**1.43**	**1.73**	putative phage protein; Antigen B protein LmaB
LMOf2365_1077	*lmo1056*	1.13	1.12	**1.51**	uncharacterized protein
LMOf2365_2689	*lmo2709*	**1.07**	**1.3**	**1.51**	uncharacterized protein
LMOf2365_0134	*lmo0116*	**1.24**	**1.41**	**1.73**	putative phage transcriptional activator, phage_ArpU superfamily; antigen C protein LmaC
LMOf2365_0197	*lmo0186*	1.01	**2.38**	**3.63**	putative resuscitation-promoting factor/stationary-phase survival autolysin, Rpf/Sps_SpsB subfamily
LMOf2365_0254	*lmo0242*	**1.18**	**1.12**	**1.59**	DUF901 superfamily protein with PIN domain
LMOf2365_2813	*lmo2822*	0.98	0.9	**1.67**	uncharacterized protein
LMOf2365_0379	*lmo0359*	0.9	**1.42**	**2.89**	putative fructose-1,6,-bisphosphate aldolase
LMOf2365_2769	*lmo2778*	0.99	1.23	**0.57**	uncharacterized protein
LMOf2365_0143	*lmo0125*	**1.28**	**1.62**	**1.94**	putative phage protein
LMOf2365_2693	*lmo2713*	1	**1.93**	**3.08**	secreted protein, COG3786 superfamily

Continued on next page

F2365 Loci	*EGD-e gene name*	pH 4.8/C	Log ratio pH 4.1/C	pH 3.5/C	Known or predicted specific function
LMOf2365_2188	*lmo2156*	0.97	**2.14**	**3.58**	YxeA family (DUF1093 superfamily) protein
LMOf2365_0431	*lmo0412*	0.97	**1.63**	**3.65**	uncharacterized membrane-associated secreted protein
LMOf2365_0037		1.03	**1.9**	**3.89**	uncharacterized protein
LMOf2365_2564	*lmo2591*	0.91	**1.86**	**3.96**	exoglucosaminidase/muramidase
LMOf2365_0346	*lmo0328*	0.92	1.11	**0.62**	uncharacterized protein
LMOf2365_0140	*lmo0122*	**1.17**	**1.43**	**1.73**	putative phage tail protein, sipho_tail superfamily
LMOf2365_0900	*lmo0881*	0.98	**1.39**	**1.8**	uncharacterized secreted protein
LMOf2365_0428	*lmo0408*	1.04	**1.31**	**1.82**	DUF1312 superfamily secreted protein
LMOf2365_2387	*lmo2416*	1.06	**1.26**	**2**	uncharacterized secreted protein
LMOf2365_1130	*lmo1124*	1.04	0.94	**2.5**	uncharacterized protein
LMOf2365_1885	*lmo1857*	0.99	1.03	**2.08**	DUF1250 (COG4479) superfamily protein
LMOf2365_1590	*lmo1568*	1.07	**1.12**	**1.53**	DUF441 superfamily protein

Note: When p value $<$ 0.05, log ratio values are in bold type.

Table 2. Comparison of the quantification results between iTRAQ and PRM of the 15 candidate proteins.

F2365 Loci	Gene name	Log ratio pH 4.8/C	iTRAQ/PRM pH 4.1/C	Results pH 3.5/C	Known or predicted specific function
LMOf2365_2702	*lmo1671*	0.98/**0.60**	**0.96/0.50**	**0.75/0.43**	zinc uptake ABC transporter, substrate-binding protein
LMOf2365_1520	*lmo1501*	**0.94/0.59**	**0.90/0.41**	**0.75/0.32**	DUF1292 superfamily protein
LMOf2365_0912	*rsbV*	**0.98**/0.64	**0.93/0.56**	**0.80/0.54**	positive (anti-sigma B) regulatory factor (acts against RsbW)
LMOf2365_1561	*rplU*	**0.96/0.63**	**0.92/0.55**	**0.80/0.50**	ribosomal protein L21
LMOf2365_2532	*lmo2560*	**0.89**/0.73	**0.94**/0.89	**0.81**/0.71	RNA polymerase, delta subunit
LMOf2365_1579	*engB*	0.98/**0.73**	0.97/**0.68**	**0.81/0.55**	ribosome assembly GTP-binding protein
LMOf2365_2603	*rplW*	**0.94/0.70**	**0.94/0.60**	**0.81/0.58**	ribosomal protein L23
LMOf2365_2148	*lmo2115*	**0.97**/0.66	**0.93**/0.59	**0.82**/0.65	putative drug/toxic substance efflux ABC transporter, permease protein
LMOf2365_1708	*lmo1684*	**0.93/0.68**	**0.90/0.51**	**0.82/0.57**	putative D-isomer 2-hydroxy acid dehydrogenase, NADB_Rossmann superfamily
LMOf2365_0140	*lmo0122*	**1.17**/1.27	**1.43**/1.70	**1.73/2.36**	putative phage tail protein, sipho_tail superfamily
LMOf2365_0136	*lmaA*	**1.13**/1.24	**1.84/4.05**	**2.09/4.97**	putative phage tail protein, phage_tail_2_superfamily; antigen A protein LmaA
LMOf2365_0213	*lmo0202*	0.97/**0.64**	**1.88**/1.89	**3.24/2.64**	listeriolysin O LLO
LMOf2365_0948	*lmo0927*	1.01/1.09	**1.98**/17.47	**3.64/45.00**	exported glycerolphosphate lipoteichoic acid synthetase
LMOf2365_2478	*lmo2505*	0.98/**0.62**	**2.31/6.62**	**3.81/18.86**	peptidoglycan DL-endopeptidase P45
LMOf2365_0611	*iap*	0.99/0.95	**1.25**/1.17	**5.56**/**11.32**	gamma-D-glutamate-meso-diaminopimelate muropeptidase; invasion-associated protein Iap

Note: When p value $<$ 0.05, log ratio value are in bold type.

None of the stress-responsive major master transcriptional regulators were affected by acidification in F2365. This is different to strain ScottA, which showed distinct responses when under sub-lethal to near lethal acid stress [10]. The hypothesis is that activation/repression of many of these regulators is transient and, by the stationary growth phase in F2365, the regulators had stable levels and thus already had cascaded downstream expression responses. There were some regulators affected in this experiment, including TetR family regulator Lmo2176 (SpxA1) and uncharacterized regulators Lmo2132 (Crp-family) and Lmo2447. SpxA1 has been found to activate genes for heme synthesis, thus influencing the expression of heme-containing proteins like catalase, enabling *L. monocytogenes* to have good aerobic growth [56]. As mentioned above, specific proteins linked to heme uptake and turnover were stimulated, as well as those associated with aerobic respiration and catabolism (e.g., QoxA, GlpK), thus these could be linked indirectly in this situation.

Numerous uncharacterized proteins or proteins with elusive functions respond to lethal acid stress (Table 1). This includes increased levels of several proteins of a decayed prophage locus (Lmo0114-0128). This set of proteins includes LmaABCD [57], which seem to be needed for good host survival despite their role remaining mysterious. The other uncharacterized proteins, all mostly having domains of unknown function or lipoproteins (e.g., Lmo0394), may have disparate but secondary roles in *L. monocytogenes*, with none being essential under standard growth conditions in rich media at 37 ℃ [58]. Only a few have any predicted enzyme function, where they could serve, for example, a remediation role in the cytoplasm removing toxic metabolites. In this respect, the azoreductase AzoR1 (Lmo0786) (studied in *E. coli* [59]) became more abundant, despite its actual substrate(s) remaining unknown for *L. monocytogenes.* Another protein, Lmo2642, is probably engaged as second messenger, being a putative cyclic nucleotide phosphodiesterase [60]; however, its role in signaling is yet to be deduced. Similarly, the function of other proteins, such as Lmo2648, which is a putative lactonase or phosphotriesterase, can only be speculated on.

4. Conclusions

Under normal circumstances, most *L. monocytogenes* strains can survive non-growth-permissive acid stress for extended periods, especially when at sub-optimal growth temperatures. For example, at 25 ℃ or lower, the strain ScottA lasts for multiple days when in a brine solution under what would be lethal acid conditions (pH 3.0 [8]). At 37 ℃, the infiltration rate of protons across the cytoplasmic membrane increases rapidly, inevitably overwhelming cytoplasmic homeostatic mechanisms, as shown for ATCC 19115 in a similar study [28]. For isolates such as 4b serotype strains ScottA, the rate of inactivation is slower than in strains like F2365. This could be due to its more robust cell wall, a feature in which F2365 is weakened due to stop codon mutations in around 20 genes [16,17]. The overall results indicate that sub-lethal and lethal acid stress in F2365 includes far fewer responses than observed in ScottA [10], and instead only includes mainly specific changes in metabolism that likely either compensate or bolster the associated processes. Data suggest that some responses seem akin to the response *L. monocytogenes* has in general when it adapts to the human host cells (for example, virulence proteins). This too was observed to occur in ScottA, including an increase in the abundance of InlB. In common to ScottA, strain F2365 showed stimulation of proteins that have major roles in the maintenance of the cell envelope, for example CwlO/Spl, Iap, and peptidoglycan turnover proteins, when experiencing severe growth inhibitory stress by acidification. One reason for these proteins being activated could simply be the flow of

sugars into the peptidoglycan monomer synthesis pathway being blocked due to lack of cell energy for synthesis. A key enzyme of glycolysis/gluconeogenesis, FbaA, was more abundant in F2365, while in ScottA the impact on the glycolysis pathway (and central metabolism) was greater in extent. This could relate to the cellular physiology being more impacted in F2365, impeding the ability to create more or rescue proteins, an energy-intensive process. In the end, the process of cell wall renewal is a basic necessity to survive under stress conditions, including in merely the stationary growth phase [61]. Once the protections created by the transition of stationary growth phase have been exceeded, as occurs when pH drops below pH 4.1, the options for F2365 seem to be very limited. It can only compensate its metabolism, which it does rather feebly compared to ScottA, which was found to much more active and widespread; instead, most efforts seems placed on futile cell wall maintenance and a last gasp attempt to escape via cell invasion.

Use of AI tools declaration

The authors declare we have not used Artificial Intelligence (AI) tools in the creation of this article.

Acknowledgments

The study was funded by Hebei Natural Science Foundation (Grant No. C2021411001) and was funded by Science Research Project of Hebei Education Department (Grant No. ZD2021001). We thank Shanghai Applied Protein Technology Co. Ltd. for providing technical support.

Conflict of interest

There is no conflict of interest for this article.

References

1. Buchanan RL, Gorris LGM, Hayman MM, et al. (2017) A review of Listeria monocytogenes: An update on outbreaks, virulence, dose-response, ecology, and risk assessments. *Food Control* 75: 1–13. https://doi.org/10.1016/j.foodcont.2016.12.016
2. Fan Z, Xie J, Li Y, et al. (2019) Listeriosis in mainland China: A systematic review. *Int J Infect Dis* 81: 17–24. https://doi.org/10.1016/j.ijid.2019.01.007
3. Bagatella S, Tavares-Gomes L, Oevermann A (2022) Listeria monocytogenes at the interface between ruminants and humans: A comparative pathology and pathogenesis review. *Vet Pathol* 59: 186–210. https://doi.org/10.1177/03009858211052659
4. Koopmans MM, Brouwer MC, Vázquez-Boland JA, et al. (2023) Human listeriosis. *Clin Microbiol Rev* 36: e0006019. https://doi.org/10.1128/cmr.00060-19
5. Lanciotti R, Braschi G, Patrignani F, et al. (2019) How *Listeria monocytogenes* shapes its proteome in response to natural antimicrobial compounds. *Front Microbiol* 10: 437. https://doi.org/10.3389/fmicb.2019.00437

6. Chen YA, Chen GW, Ku HH, et al. (2022) Differential proteomic analysis of *Listeria monocytogenes* during high-pressure processing. *Biology* 11: 1152. https://doi.org/10.3390/biology11081152
7. D'Onofrio F, Schirone M, Krasteva I, et al. (2023) A comprehensive investigation of protein expression profiles in *L. monocytogenes* exposed to thermal abuse, mild acid, and salt stress conditions. *Front Microbiol* 14: 1271787. https://doi.org/10.3389/fmicb.2023.1271787
8. Zhang DL, Ross T, Bowman JP (2010) Physiological aspects of *Listeria monocytogenes* during inactivation accelerated by mild temperatures and otherwise non-growth permissive acidic and hyperosmotic conditions. *Int J Food Microbiol* 141: 177–185.
9. Zhang DL, McQuestin OJ, Mellefont LA, et al. (2010) The influence of non-lethal temperature on the rate of inactivation of vegetative bacteria in inimical environments may be independent of bacterial species. *Food Microbiol* 27: 453–459.
10. Bowman JP, Hages E, Nilsson RE, et al. (2012) Investigation of the *Listeria monocytogenes* Scott A acid tolerance response and associated physiological and phenotypic features via whole proteome analysis. *J Proteome Res* 11: 2409–2426.
11. Manso B, Melero B, Stessl B, et al. (2020) The response to oxidative stress in *Listeria monocytogenes* is temperature dependent. *Microorganisms* 8: 521. https://doi.org/10.3390/microorganisms8040521
12. Pittman JR, Buntyn JO, Posadas G, et al. (2014) Proteomic analysis of cross protection provided between cold and osmotic stress in *Listeria monocytogenes*. *J Proteome Res* 13: 1896–1904.
13. Melian C, Castellano P, Segli F, et al. (2021) Proteomic analysis of *Listeria monocytogenes* fbunt during biofilm formation at 10 °C in response to lactocin AL705. *Front Microbiol* 12: 604126. https://doi.org/10.3389/fmicb.2021.604126
14. Shabala L, Lee SH, Cannesson P, et al. (2008) Acid and NaCl limits to growth of *Listeria monocytogenes* and influence of sequence of inimical acid and NaCl levels on inactivation kinetics. *J Food Protect* 71: 1169–1177. https://doi.org/10.4315/0362-028x-71.6.1169
15. Ross T, Zhang D, McQuestin O (2008) Temperature is the main factor governing the rate of non-thermal inactivation of vegetative bacteria. *Int J Food Microbiol* 128: 129–135.
16. Nightingale KK, Milillo SR, Ivy RA, et al. (2007) *Listeria monocytogenes* F2365 carries several authentic mutations potentially leading to truncated gene products, including inlB, and demonstrates atypical phenotypic characteristics. *J Food Protect* 70: 482–488. https://doi.org/10.4315/0362-028x-70.2.482
17. Oliver HF, Orsi RH, Wiedmann M, et al. (2013) σ(B) plays a limited role in the ability of *Listeria monocytogenes* strain F2365 to survive oxidative and acid stress and in its virulence characteristics. *J Food Protect* 76: 2079–2086. https://doi.org/10.4315/0362-028X.JFP-12-542
18. Qin X, He S, Zhou X, et al. (2019) Quantitative proteomics reveals the crucial role of YbgC for Salmonella enterica serovar Enteritidis survival in egg white. *Int J Food Microbiol* 289: 115–126.
19. Wisniewski JR., Zougman A, Nagaraj N, et al. (2009) Universal sample preparation method for proteome analysis. *Nat Methods* 6: 359–362.
20. Ashburner M, Ball CA, Blake JA, et al. (2000). Gene ontology: Tool for the unification of biology. The Gene Ontology Consortium. *Nat Genet* 25: 25–29.
21. Gotz S, García-Gómez JM, Terol J, et al. (2008) High-throughput functional annotation and data mining with the last2GO suite. *Nucleic Acids Res* 36: 3420–3435.

22. Kanehisa M, Goto S, Sato Y, et al. (2012) KEGG for integration and interpretation of large-scale molecular data sets. *Nucleic Acids Res* 40: D109–D114.
23. Peterson AC, Russell JD, Bailey DJ, et al. (2012) Parallel reaction monitoring for high resolution and high mass accuracy quantitative, targeted proteomics. *Mol Cell Proteomics* 11: 1475–1488.
24. MacLean B, Tomazela DM, Shulman N, et al. (2010) Skyline: An open source document editor for creating and analyzing targeted proteomics experiments. *Bioinformatics* 26: 966–968. https://doi.org/10.1093/bioinformatics/btq054
25. Melo J, Schrama D, Hussey S, et al. (2013) Listeria monocytogenes dairy isolates show a different proteome response to sequential exposure to gastric and intestinal fluids. *Int J Food Microbiol* 163: 51–63. https://doi.org/10.1016/j.ijfoodmicro.2013.03.001
26. Chen GW, Chen YA, Chang HY, et al. (2021) Combined impact of high-pressure processing and slightly acidic electrolysed water on *Listeria monocytogenes* proteomes. *Food Res Int* 147: 110494. https://doi.org/10.1016/j.foodres.2021.110494
27. D'Onofrio F, Schirone M, Paparella A, et al. (2023) Stress adaptation responses of a *Listeria monocytogenes* 1/2a strain via proteome profiling. *Foods* 12: 2166. https://doi.org/10.3390/foods12112166
28. Zhang D, Bai YL, Bowman JP (2019) Impact of combined acidic and hyperosmotic shock conditions on the proteome of *Listeria monocytogenes* ATCC 19115 in a time-course study. *J Food Quality* 2019: 3075028. https://doi.org/10.1155/2019/3075028
29. Guan N, Liu L (2020) Microbial response to acid stress: mechanisms and applications. *Appl Microbiol Biotech* 104: 51–65. https://doi.org/10.1007/s00253-019-10226-1
30. Korovila I, Hugo M, Castro JP, et al. (2017) Proteostasis, oxidative stress and aging. *Redox Biol* 13: 550–567. https://doi.org/10.1016/j.redox.2017.07.008
31. Schramm FD, Schroeder K, Jonas K (2020) Protein aggregation in bacteria. *FEMS Microbiol Rev* 44: 54–72. https://doi.org/10.1093/femsre/fuz026
32. Rothman JE, Schekman R (2011) Molecular mechanism of protein folding in the cell. *Cell* 146: 851–854. https://doi.org/10.1016/j.cell.2011.08.041
33. Izquierdo-Fiallo K, Muñoz-Villagrán C, Orellana O, et al. (2023) Comparative genomics of the proteostasis network in extreme acidophiles. *PLoS ONE* 18: e0291164. https://doi.org/10.1371/journal.pone.0291164
34. Grubaugh D, Regeimbal JM, Ghosh P, et al. (2018) The VirAB ABC transporter is required for *virR* regulation of *Listeria monocytogenes* virulence and resistance to nisin. *Infect Immun* 86: e00901-17. https://doi.org/10.1128/IAI.00901-17
35. Engelgeh T, Herrmann J, Jansen R, et al. (2023) Tartrolon sensing and detoxification by the *Listeria monocytogenes timABR* resistance operon. *Mol Microbiol* 120: 629–644. https://doi.org/10.1111/mmi.15178
36. Brodiazhenko T, Turnbull KJ, Wu KJY, et al. (2022) Synthetic oxepanoprolinamide iboxamycin is active against *Listeria monocytogenes* despite the intrinsic resistance mediated by VgaL/Lmo0919 ABCF ATPase. *JAC Antimicrob Resist* 4: dlac061. https://doi.org/10.1093/jacamr/dlac061
37. Reniere ML, Ukpabi GN, Harry SR, et al. (2010) The IsdG-family of haem oxygenases degrades haem to a novel chromophore. *Mol Microbiol* 75: 1529–1538.

38. Perveen S, Rashid N, Tang XF, et al. (2017) Anthranilate phosphoribosyltransferase from the hyperthermophilic archaeon Thermococcus kodakarensis shows maximum activity with zinc and forms a unique dimeric structure. *FEBS Open Bio* 7: 1217–1230.
39. Krishna Kumar VG, Paul A, Gazit E, et al. (2018) Mechanistic insights into remodeled Tau-derived PHF6 peptide fibrils by naphthoquinone-tryptophan hybrids. *Sci Rep* 8: 71.
40. Grubmüller S, Schauer K, Goebel W, et al. (2014) Analysis of carbon substrates used by *Listeria monocytogenes* during growth in J774A.1 macrophages suggests a bipartite intracellular metabolism. *Front Cell Infect Microbiol* 4: 156. https://doi.org/10.3389/fcimb.2014.00156
41. Pirovich DB, Da'dara AA, Skelly PJ (2021) Multifunctional Fructose 1,6-Bisphosphate Aldolase as a Therapeutic Target. *Front Mol Biosci* 8: 719678. https://doi.org/10.3389/fmolb.2021.719678
42. Wang G, Xia Y, Cui J, et al. (2014) The roles of moonlighting proteins in bacteria. *Curr Issues Mol Biol* 16: 15–22.
43. Paspaliari DK, Kastbjerg VG, Ingmer H, et al. (2017) Chitinase expression in *Listeria monocytogenes* is influenced by lmo0327, which encodes an internalin-like protein. *Appl Environ Microbiol* 83: e01283-17
44. Sannino DR, Kraft CE, Edwards KA, et al. (2018) Thiaminase I provides a growth advantage by salvaging precursors from environmental thiamine and its analogs in *Burkholderia thailandensis.* *Appl Environ Microbiol* 84: e01268-18. https://doi.org/10.1128/AEM.01268-18
45. Corbett D, Goldrick M, Fernandes VE, et al. (2017) *Listeria monocytogenes* has both cytochrome bd-type and cytochrome aa3-type terminal oxidases, which allow growth at different oxygen levels, and both are important in infection. *Infect Immun* 85: e00354-17. https://doi.org/10.1128/IAI.00354-17
46. Gouin E, Adib-Conquy M, Balestrino D, et al. (2010). The *Listeria monocytogenes* InlC protein interferes with innate immune responses by targeting the IκB kinase subunit IKKα. *PNAS* 107: 17333–17338. https://doi.org/10.1073/pnas.1007765107
47. Garandeau C, Réglier-Poupet H, Dubail I, et al. (2002). The sortase SrtA of *Listeria monocytogenes* is involved in processing of internalin and in virulence. *Infect Immun* 70: 1382–1390. https://doi.org/10.1128/IAI.70.3.1382-1390.2002
48. Reniere ML, Whiteley AT, Hamilton KL, et al. (2015) Glutathione activates virulence gene expression of an intracellular pathogen. *Nature* 517: 170–173. https://doi.org/10.1038/nature14029
49. Gaballa A, Guariglia-Oropeza V, Wiedmann M, et al. (2019) Cross talk between SigB and PrfA in *Listeria monocytogenes* facilitates transitions between extra-and intracellular environments. *Microbiol Mol Biol Rev* 83: e00034-19. https://doi.org/10.1128/MMBR.00034-19
50. Pinto D, São-José C, Santos MA, et al. (2013) Characterization of two resuscitation promoting factors of *Listeria monocytogenes*. *Microbiology* 159: 1390–1401. https://doi.org/10.1099/mic.0.067850-0
51. Dell'Era S, Buchrieser C, Couvé E, et al. (2009) *Listeria monocytogenes* L-forms respond to cell wall deficiency by modifying gene expression and the mode of division. *Mol Microbiol* 73: 306–322. https://doi.org/10.1111/j.1365-2958.2009.06774.x
52. Alharbi MAS (2018) Aging and recovery of Listeria monocytogenes ScottA. PhD Thesis, University of Tasmania.

53. Györkei Á, Daruka L, Balogh D, et al. (2022) Proteome-wide landscape of solubility limits in a bacterial cell. *Sci Rep* 12: 6547. https://doi.org/10.1038/s41598-022-10427-1
54. Santos T, Viala D, Chambon C, et al. (2019) *Listeria monocytogenes* biofilm adaptation to different temperatures seen through shotgun proteomics. *Front Nutr* 6: 89. https://doi.org/10.3389/fnut.2019.00089
55. Kamp HD, Higgins DE (2011) A protein thermometer controls temperature-dependent transcription of flagellar motility genes in *Listeria monocytogenes*. *PLOS Pathogens* 7: e1002153. https://doi.org/10.1371/journal.ppat.1002153
56. Cesinger MR, Thomason MK, Edrozo MB, et al. (2020). *Listeria monocytogenes* SpxA1 is a global regulator required to activate genes encoding catalase and heme biosynthesis enzymes for aerobic growth. *Mol Microbiol* 114: 230–243
57. Fox EM, Allnutt T, Bradbury MI, et al. (2016) Comparative genomics of the *Listeria monocytogenes* ST204 Subgroup. *Front Microbiol* 7: 2057. https://doi.org/10.3389/fmicb.2016.02057
58. Fischer MA, Engelgeh T, Rothe P, et al. (2022*). Listeria monocytogenes* genes supporting growth under standard laboratory cultivation conditions and during macrophage infection. *Genome Res* 32: 1711–1726. https://doi.org/10.1101/gr.276747.122
59. Cui D, Li G, Zhao D, et al. (2015) Effect of quinoid redox mediators on the aerobic decolorization of azo dyes by cells and cell extracts from Escherichia coli. *Environ Sci Pollut Res Int* 22: 4621–4630. https://doi.org/10.1007/s11356-014-3698-6
60. Kim YG, Jeong JH, Ha NC, et al. (2011) Structural and functional analysis of the Lmo2642 cyclic nucleotide phosphodiesterase from *Listeria monocytogenes*. *Proteins* 79: 1205–1214. https://doi.org/10.1002/prot.22954
61. Borisova M, Gaupp R, Duckworth A, et al. (2016) Peptidoglycan recycling in Gram-Positive bacteria Is crucial for survival in stationary phase. *mBio* 7: e00923-16. https://doi.org/10.1128/mBio.00923-16

Supplementary

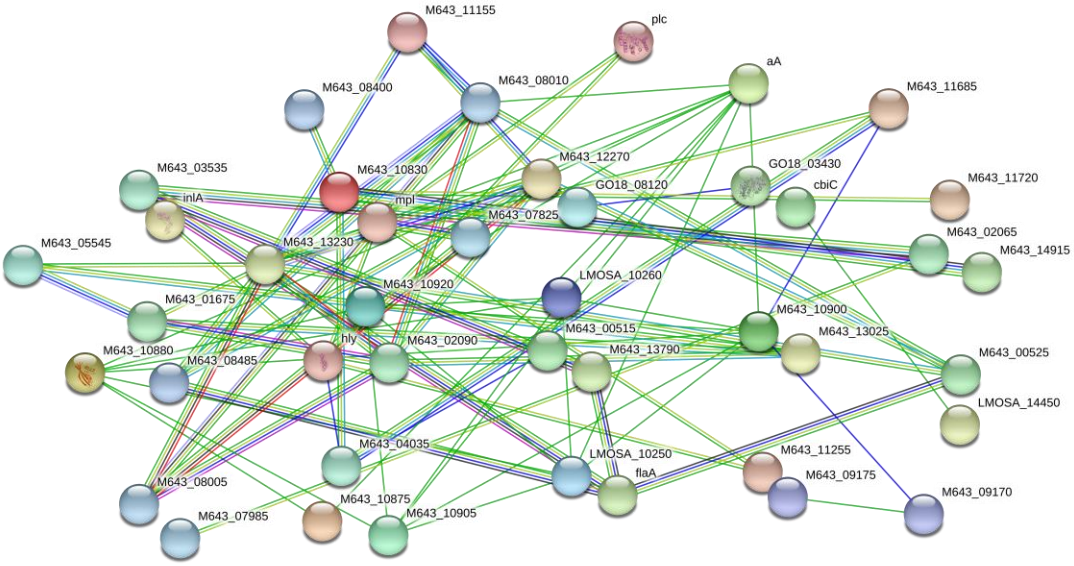

Figure S1. Network diagram showing the co-occurrence of responsive proteins to progressive medium acidification (adjusted with HCl solution of pH 3.0. 5 min: pH 4.8; 1 h: pH 4.1; 2 h: pH 3.5) on *Listeria monocytogenes* F2365 grown in TSB-YE at 37 ℃. Nodes are individual proteins of strain F2635. The edges indicate significant correlations (minimum 0.4) between proteins in terms of changes in responses to growth medium acidification. The lines are edges that are color-coded to show the nature of the relationships—green line: neighborhood proteins; blue line: co-occurrence evidence; purple line: experimental evidence; yellow line: text-mining evidence; black line: co-expression evidence.

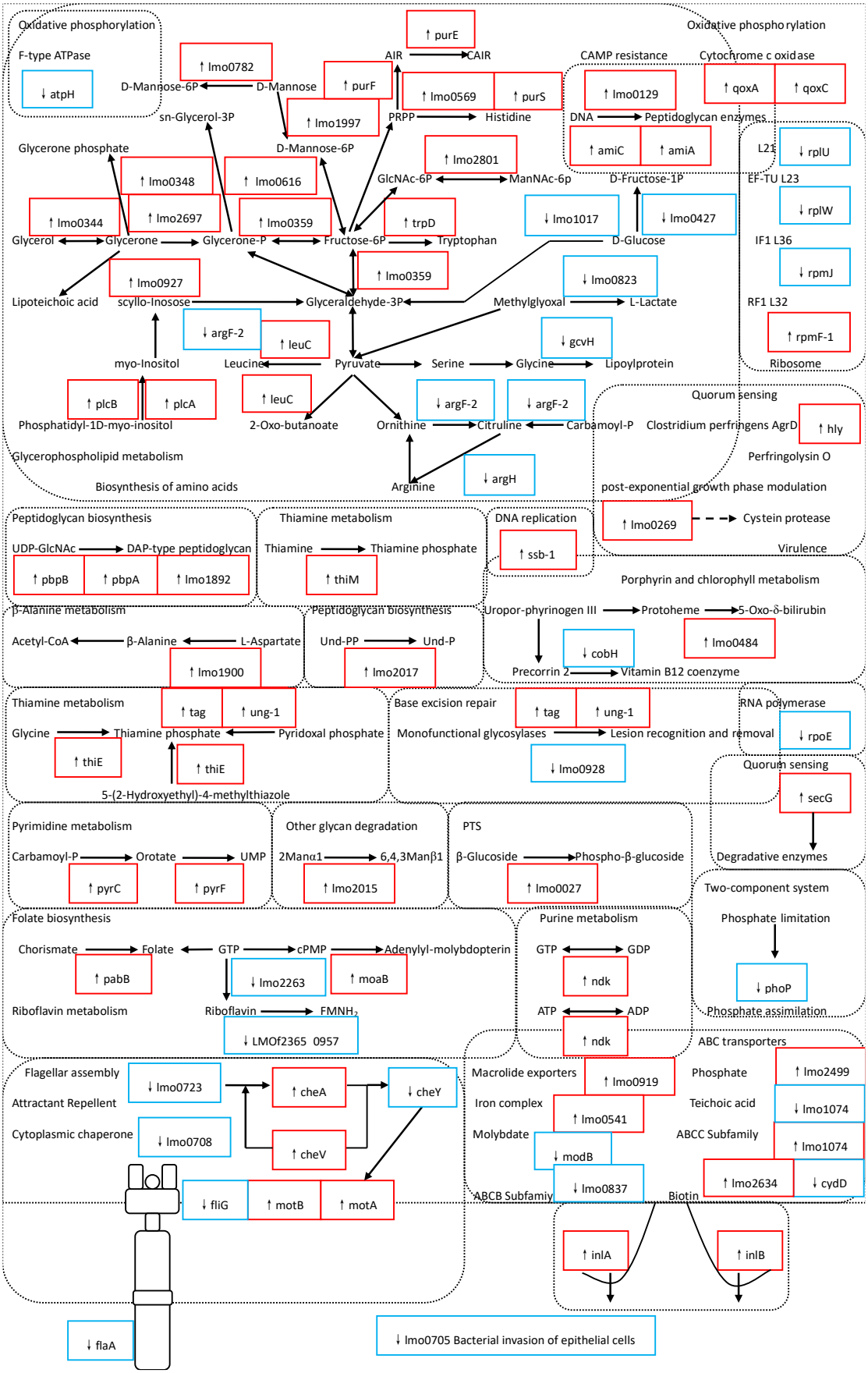

Figure S2. Metabolic pathway map of protein change responses of *Listeria monocytogenes* F2365 to progressive medium acidification (adjusted with HCl solution of pH 3.0. 5 min: pH 4.8; 1 h: pH 4.1; 2 h: pH 3.5) grown in TSB-YE at 37 °C.

AIMS Press